

Review

## Repassivation Kinetics and its Role in SCC Prediction- A Review

Ihsan-ul-Haq Toor

Dept. of Mechanical Engineering, King Fahd University of Petroleum & Minerals (KFUPM)  
Dhahran 31261, Kingdom of Saudi Arabia  
E-mail: [ihsan@kfupm.edu.sa](mailto:ihsan@kfupm.edu.sa), [ihsan\\_jut@hotmail.com](mailto:ihsan_jut@hotmail.com)

Received: 29 December 2013 / Accepted: 5 February 2014 / Published: 23 March 2014

This paper reviews the relationship between repassivation kinetics and stress corrosion cracking (SCC) susceptibility of materials in terms of *cBV* model developed using rapid scratch electrode technique (RSET). In this technique repassivation kinetics of the alloys was analyzed in terms of the current density flowing from the scratch,  $i(t)$ , as a function of the charge density that has flowed from the scratch,  $q(t)$ . Repassivation on the scratched surface of the alloys occurred in two kinetically different processes; passive film initially nucleated and grew according to the place exchange model in which  $\log i(t)$  is linearly proportional to  $q(t)$ , and then grew according to the high-field ion conduction model in which  $\log i(t)$  is linearly proportional to  $1/q(t)$ . The slope determined from the  $\log i(t)$  versus  $1/q(t)$  plot (called *cBV*) was found to be a parameter representing the repassivation rate, stress corrosion cracking (SCC) susceptibility and protectiveness of the passive film.

**Keywords:** Repassivation kinetics, Stress corrosion cracking, Scratch test, Inhibitors, Stainless steels

### 1. INTRODUCTION

Stainless steels (SSs) and Ni-based alloys are being used extensively in the modern day industrial society, even though these metals are spontaneously oxidized by reacting with water and/or oxygen in terrestrial environments. So in spite of their high thermodynamic reactivity, it is the phenomenon of passivity which is responsible for their stability [1]. This kinetic stability is due to the formation of a “passive” film on the surface that effectively isolates the reactive metal from the corrosive environment, as was originally postulated by Faraday [2]. The quality of this passive film in terms of its ion- and electron-transport properties, or in terms of its structure and chemistry is responsible for the corrosion resistance of metal and alloys [3, 4].

The co-relation between passivity and corrosion resistance can be understood by the fact that almost 30% cases of corrosion failures are caused by localized corrosion (localized breakdown of the passive film) including pitting corrosion and stress corrosion cracking (SCC). SCC is a brittle fracture at relatively low constant tensile stress of an alloy exposed to corrosive environment. Unexpected occurrence of SCC in various industrial applications has caused major corrosive damages. Many mechanistic models have been developed to understand and mitigate SCC but a lot of problems are still unresolved. One of the very important and interesting issues in the mechanism of SCC is the initiation process, because failure life is not decided by the growth or propagation, but mainly by the initiation of cracks. The breakdown of passive film both mechanically or chemically, has been one of the most important issues in the passivity theory and is also important in understanding SCC initiation process.

The severity of SCC has driven researchers to develop various testing techniques in order to evaluate the susceptibility towards SCC. One of the candidates for this is the measurement of repassivation kinetics. The repassivation is a film reforming process on the broken surface film, and hence its kinetics has been considered to be a critical factor in determining the SCC susceptibility of an alloy [5, 6]. The general relationship between the repassivation rate and SCC susceptibility has been explained by the slip dissolution model [6-8]. According to this model crack initiate and propagate by repetitive processes of slip induced film rupture /dissolution /repassivation. SCC cracks initiate and propagate at intermediate repassivation rates. The inherent repassivation rate of an alloy depends upon the solution temperature, pH, chloride concentration, applied potential, and the chemical composition of the alloy. The film rupture rate depends on loading condition and microstructure of the alloy, thus, for an alloy/environment system subjected to deforming at a constant strain rate or to a constant loading condition, the inherent repassivation rate of the alloy measured without applied stress should determine the SCC susceptibility. Based on the high field ion conduction model, Kwon et al. [9] proposed a repassivation parameter characterizing the repassivation rate of an alloy, and developed a model (cBV model) to predict SCC susceptibility of SSs in terms of this repassivation parameter. So here in this paper, a detailed review of the recently published literature in which cBV model was successfully applied to predict SCC susceptibility of different materials such as SSs, Ni base alloys and inhibitors etc. is presented.

## 2. DESCRIPTION OF cBV MODEL AND ITS RELATION TO SCC

Since SCC occurs by slip dissolution model, a repetitive process of film breakdown–dissolution–repassivation [10, 11], so repassivation kinetics of a broken film surface of an alloy is of critical importance [5, 6]. Kinetics of film reforming process is related closely to the initiation and propagation of SCC. Passive films can be fractured by chemical attack of halide ions especially chloride ions or by slip step extrusion under tensile stress or by the impact of particles in solution. If environments (temp., applied potential, solution composition, creep rate etc.) permit, the passive film reforms by oxidation of the bare metal surface. Once the passive film is fractured, oxidation of the bare metal surface proceeds leading to localized corrosion till oxide film is covered again. Localized

corrosion, i.e. crevice corrosion, pitting, SCC and corrosion fatigue under tensile stress is closely related to repassivation kinetics [12-16]. To study the repassivation behavior, artificial breakdown of the passive film is required.

Simulation of the passive film breakdown under various environments has been done by straining electrode methods [17, 18], abrading method [19, 20], in-situ fracture methods [21] and scratching electrode method [22-24]. Once the film is fractured current density abruptly increases to the peak, thereafter decreased again due to repassivation process. Current flowed during repassivation has important meaning in characterizing SCC and this current must be analyzed to explain the relationship between repassivation kinetics and SCC.

## 2.1 Rapid Scratch Electrode Technique (RSET)

Kwon et al. [9] used rapid scratch electrode technique (RSET) for repassivation kinetics studies. They devised an electrochemical cell to measure the repassivation current on the rapidly scratched surface of the materials as shown in Fig. 1.

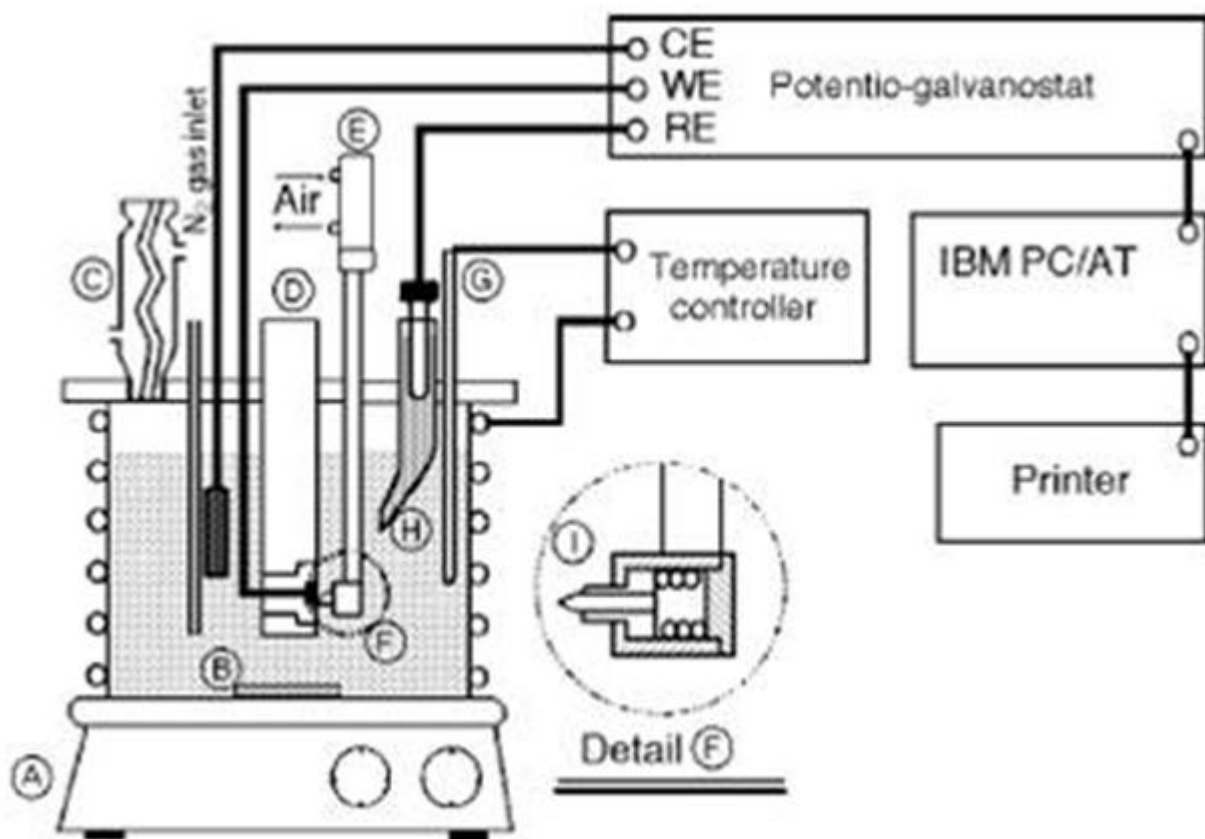


**Figure 1.** Experimental system with a corrosion cell modified for scratching electrode test, where A is the magnetic plate, B is the stirrer, C is the condenser, D is the specimen holder, E is the solenoid valve, F is the scratcher, G is the thermometer, H is the Luggin probe, and I is the diamond tip. CE, WE, and RE denote counter electrode, working electrode, and reference electrode, respectively. [Source: Ref. 9]

The cell consisted of a specimen as a working electrode, platinum as a counter electrode and saturated calomel electrode (SCE) positioned in a salt bridge as a reference electrode, and a scratcher with alumina tip. To rupture the passive film by scratch, an alumina tip loaded on a spring was pulled rapidly up along the surface of the specimen fixed into the specimen holder by an air pressure cylinder connected to a solenoid valve. The surface of the sample was scratched under potentiostatic condition after formation of a stable passive film, and current flow from the scratch was measured every millisecond during and after the scratching, and computer-processed for further analysis.

For typical current transient of SSs, two models of Sato and Cohen [25] and Cabrera and Mott [26] provided the base for exploring variables and laws governing repassivation of alloys. According to the place exchange model proposed by Sato and Cohen [25], a layer of oxygen is adsorbed onto the surface and then exchanges places (possibly by rotation) with underlying metal atoms. A second layer of oxygen is adsorbed and the two M-O pairs rotate simultaneously. This process is repeated and results in the formation of oxide film. Based on this model, it was deduced that logarithms of anodic current density ( $i(t)$ ) are linearly proportional to charge density ( $q(t)$ ) that has flowed from the scratch during repassivation;

$$\log i(t) = \log k' + \beta V - \frac{q(t)}{K} \quad (1)$$

where,  $k'$  and  $K$  are constants,  $V$  is the applied potential and  $q(t)$  is experimentally determined by integration of the current density with time during the repassivation. According to the high field ion conduction model, the passive film grows by the transport of metal ions across the film toward the film/electrolyte interface under high electric fields of a few MV/cm, and thus, the ion conduction rate through the film during repassivation is expressed by the current represented by Eq. 2;

$$i(t) = A \exp[BV/h(t)] \quad (2)$$

where  $A$  and  $B$  are parameters associated with the activation energy for mobile ion migration,  $V$  is the potential drop across the film whose thickness is  $h(t)$ .

The anodic current measured on the scratched surface during repassivation is consumed for two anodic processes; one is metal dissolution reaction, and the other is repassivation that is an oxidation reaction of metal with water to form the passive film. Burstein and Marshall [27] clearly demonstrated that for SSs in chloride solution, the anodic current measured during repassivation is mostly consumed to form passive film on the scratched surface as far as the metal dissolution does not become dominant by pitting or general corrosion, and hence the anodic current associated with the metal dissolution is negligibly small. Thus, by neglecting the current associated with the metal dissolution, the charge density ( $q(t)$ ) that has flowed from the scratch during repassivation has the following relationship with the film thickness ( $h(t)$ );

$$q(t) = \frac{zF\rho}{M} h(t) \quad (3)$$

where  $z$  is the number of electrons transferred for an ion,  $F$  is the Faraday constant,  $\rho$  is the film density, and  $M$  is the molecular mass of film.

Combining Eqs. 2 and 3 yields Eq. 4;

$$\log i(t) = \log A + \frac{BVzF\rho}{2.3Mq(t)} = \log A + \frac{cBV}{q(t)} \quad (4)$$

According to Eq. 4,  $\log i(t)$  is linearly proportional to the  $1/q(t)$  with the slope of cBV, where the c is a constant equal to  $zFp/2.3M$ . The value of c can be calculated for ferritic SSs by considering that  $z = 3$ ,  $\rho = 5.24 \text{ g/cm}^2$  ( $\rho(\text{Fe}_2\text{O}_3) = 5.27 \text{ g/cm}^2$ ,  $\rho(\text{Cr}_2\text{O}_3) = 5.21 \text{ g/cm}^2$ ),  $M = 156 \text{ g/mol}$  ( $M(\text{Fe}_2\text{O}_3) = 160 \text{ g/mol}$ ,  $M(\text{Cr}_2\text{O}_3) = 152 \text{ g/mol}$ ) [27]. Quantitative criterion for the susceptibility to SCC, however, has been remained obscure and considerable additional work needs to be performed to provide better definition and justification for correlation between current transient curve and SCC behavior. Kwon et al. [9, 28, 29] employed the repassivation kinetics to predict the resistance to SCC susceptibility and introduced a new parameter called “cBV” based on high-field ion conduction model. According to them, with an increase in cBV value, repassivation rate of an alloy is decreased and hence the resistance to SCC decreases as well. Moreover, they found one to one agreement in the prediction of SCC with cBV value in SSs with variation in temperature, chloride concentration and alloy compositions. According to the Kwon’s cBV model, the following steps are needed to predict the SCC susceptibility of the alloy/environment system;

- Measure current transient curves for a given alloy/environment system under potentiostatic condition using a rapid scratch electrode technique as shown Fig. 2 (a) and (b).

•

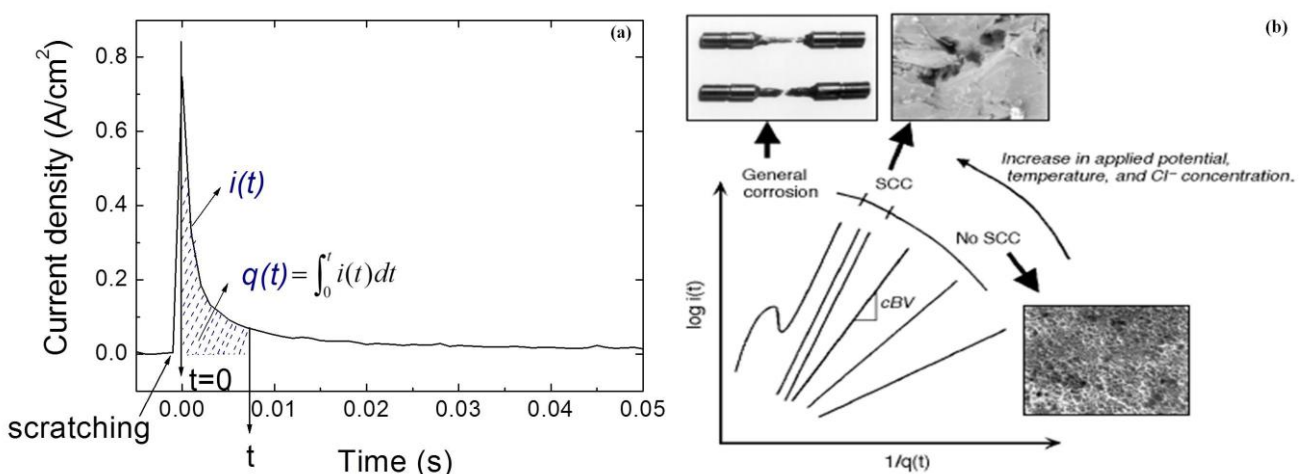


**Figure 2.** (a) Typical transient of RSET along (b) Schematic representation of the relationship between  $cBV$  value and SCC susceptibility [Source: Ref. 9]

- Do similar work with an increase in applied potential, or in solution temperature or in chloride concentration
- Draw  $\log i(t)$  vs  $1/q(t)$  plots with an increase in applied potential, or in solution temperature or in chloride concentration using the data in the current transient curves, where  $i(t)$  is current density flowing from the scratch, and  $q(t)$  is charge density that has flowed from the scratch.
- Determine the slope (cBV) in the linear part of the  $\log i(t)$  vs  $1/q(t)$  plot, and plot cBV as a function of  $E_{app}$ , or solution temperature T, or chloride concentration [Cl].
- Dissolution mode of the alloy exposed to chloride solution under loading condition is classified into one of the following cases;

Case 1: when cBV increases with  $\uparrow E_{app}$ , or  $\uparrow T$ , or  $\uparrow [Cl^-]$  the alloy is immune to SCC.

Case 2: when cBV converges to a limiting value, SCC does occur in the alloy.

Case 3: when an inflection point appears in the  $\log i(t)$  vs  $1/q(t)$ , Severe dissolution will occur in the alloy.

### 3. APPLICATION OF cBV MODEL

Kwon's cBV model was successfully applied in many investigations to predict the SCC susceptibility of materials based on repassivation kinetics. Toor et al. [30] applied cBV model to investigate the effect of Mn on the SCC susceptibility of Mn containing SSs and results of these high Mn alloys were compared with that of conventional 304 SS alloy. High Mn-N austenitic SSs are being developed to replace high-cost Ni with low-cost Mn and N without compromising their corrosion resistance properties. These high Mn SSs contain 6–11 wt % Mn which is seven to eight times cheaper than Ni [31–36], however Mn is not as effective  $\gamma$ -stabilizer as Ni. This later problem can be solved by combining Mn with N in these SS alloys, which not only function as an austenite stabilizer but also improves resistance to localized corrosion [37]. However it is reported that Mn alone causes a significant degradation in corrosion resistance of SSs mainly due to the formation of manganese sulfide (MnS) inclusions [38–41] and others found that Mn has a detrimental effect on the general corrosion of SSs [42, 43]. Mn containing alloys are found to be extremely sensitive to the presence of minor constituents such as C, N, S, and P etc. [44].

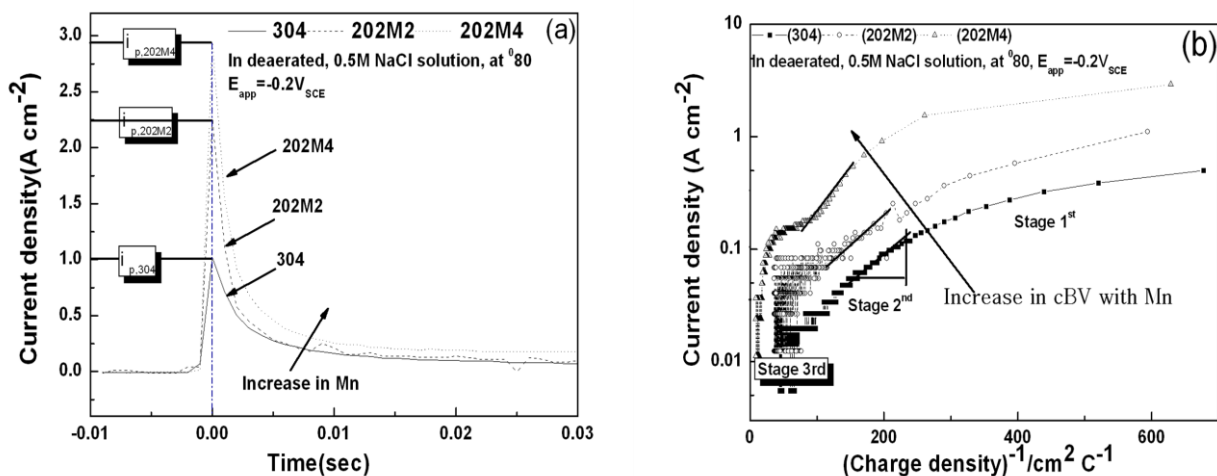


**Figure 3.** (a) Current transients for 202M2 and 202M4 alloys along with 304 SS, in deaerated 0.5M NaCl solution at 80 °C and, (b)  $\log i(t)$  vs.  $1/q(t)$  plots drawn based on the data in current transients in Fig. 5(a) to get the cBV value. [Source: Ref. 30]

In this paper, Toor et al. employed RSET to measure the repassivation kinetics of Mn containing alloys in 0.5M NaCl solution at 80 °C. Passive film was formed for 30 minutes at a stable

potential of  $-0.2V_{SCE}$  in the passive region, before it was scratched by a scratcher. As the film was scratched, anodic current density flowing from the scratch increased abruptly to a peak value due to an anodic oxidation reaction occurring on the bare surface of the alloy, and thereafter decreased as repassivation occurs as shown in Fig. 3(a). Repassivation behavior of these Mn containing SSs was analyzed based on the relationship between current density  $i(t)$  and charge density  $q(t)$  that has flown from the scratch. It was found that passive film initially nucleated according to the place exchange model, and then grew according to the high field ion conduction model in which  $\log i(t)$  vs.  $1/q(t)$  has a linear relationship with a slope ( $cBV$ ). As reported by Kwon et al. [9], that  $cBV$ , determined from the slope of  $\log i(t)$  vs.  $1/q(t)$  is a quantitative measure of repassivation rate of passive film, and closely related with SCC susceptibility of SSs in chloride solution. The lower the value of  $cBV$  for a given alloy/environment system, the faster is the repassivation of the alloy through formation of a thinner and more protective film, and thereby exhibiting less susceptibility to SCC. Figs. 3 (a) and (b) show the comparison of peak current density (current vs. time transients) and  $cBV$  (slope of  $\log i(t)$  vs.  $1/q(t)$  plot) values of the two Mn containing alloys along together with standard 304 SS alloy. It is clear that peak current density of the current transient curves (Fig. 3 (a)) was increased with an increase in Mn content of the alloys, which means that with the increase in Mn content, oxidation current of the bare metal surface was also increased. Fig. 3(b) shows that the  $cBV$  value, determined from the slope of  $\log i(t)$  vs.  $1/q(t)$  plot, was increased with an increase in Mn content of the alloys. Based on  $cBV$  value increase, Toor et al. predicted that that Mn will increase SCC susceptibility of Mn containing alloys as compared to SS304. They suggested that the addition of Mn has slowed down the repassivation kinetics by forming thicker and less protective passive films on Mn containing alloy.

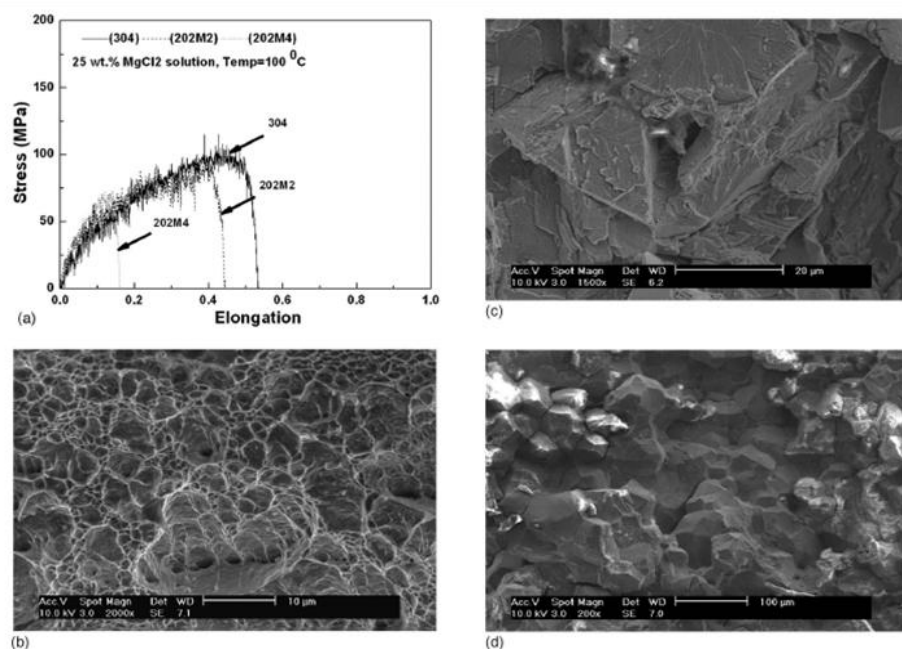


**Figure 4.** (a) Load elongation curves for the alloys at  $100^{\circ}C$  by SSRT in deaerated 25 wt %  $MgCl_2$  solution, together with their corresponding SEM fractographs. 202M4 (4(b)) exhibiting an intergranular fracture mode, while 202M2 (4(c))and 304 (4(d))show brittle and ductile rupture, respectively. [Source: Ref. 30]

However to confirm the cBV model prediction, SCC experiments were carried out in slow strain rate testing (SSRT) machine in 25 wt. % MgCl<sub>2</sub> at different temperatures (80~120 °C). Load elongation curves of SSRT experiment carried out at 100°C show that the elongation of Mn containing alloys was decreased considerably (Fig. 4a) and it was expected that alloy 202M4 may have fractured by SCC. SEM fractographs shown in Fig. 4(c) confirmed that alloy 202M4 was fractured by SCC, as it shows a typical quasi-cleavage SCC fracture (transgranular and intergranular), while the other two alloys, 202M2 and 304, showed brittle and ductile fracture, as is clear in Figs. 4(d) and 4(b) respectively. So these results are in agreement with those predicted by cBV model, that with an increase in Mn content of the alloys, SCC susceptibility was also increased.

In a recent study, Park et al. [45] investigated the independent effect of Mn on the repassivation kinetics in terms of cBV model. As mentioned above formation of MnS inclusions reduces the corrosion resistance of Mn containing SSs, so in this work they have prepared the Mn containing alloys using the vacuum refining technology such as argon oxygen decarburization (AOD) and vacuum oxygen decarburization (VOD) processes to decrease the sulphur content. Also in this study authors prepared the alloy with only Mn addition in order to study the independent effect of Mn. So when the effects of MnS as well as other alloying elements are excluded, then it would have been interesting to investigate the independent effect of Mn on cBV (repassivation kinetics), which will be then correlated with SCC susceptibility. So for this purpose authors prepared high purity Fe–18Cr–xMn (x = 0, 6, 12) alloys by vacuum arc melting for the RSET. Prior to the tests, specimen was cathodically cleaned at  $-1.0 V_{SCE}$  for 180 s. After 30 min of passivation at  $-0.1 V_{SCE}$  in 0.1M NaCl solution, passive film was broken by scratching with a sharp alumina tip at the passivation potential.

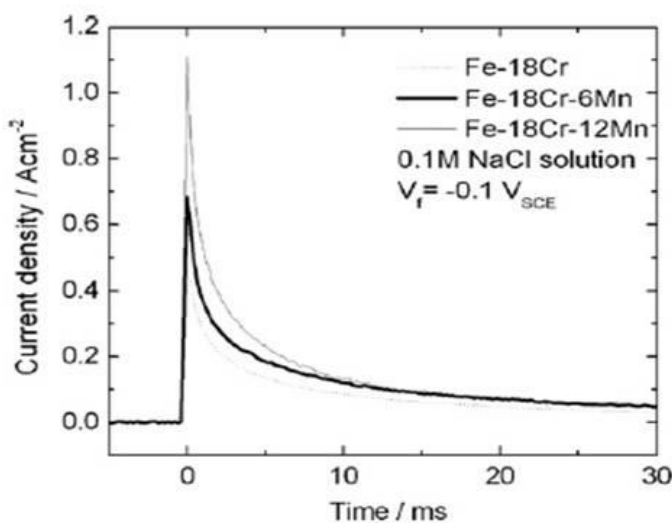


**Figure 5.** Effects of Mn content on the current transient curves of Fe–18Cr–xMn(x=0, 6, 12) during repassivation in 0.1MNaCl solution at an applied potential of  $-0.1 V_{SCE}$ . [Source: Ref. 45]

Fig. 5 shows the current transient curves when a scratch was made on the surface of the specimens. Once the film was broken by scratching the surface of the specimens, the anodic current increased abruptly to a peak due to an anodic oxidation reaction on the bare surface of the metal, and

thereafter decreased as repassivation proceeded. With an increase in Mn content of the alloys, the current peak intensity increased due to an increased oxidation tendency at the bare metal, and repassivation occurred at different rates depending on Mn content.

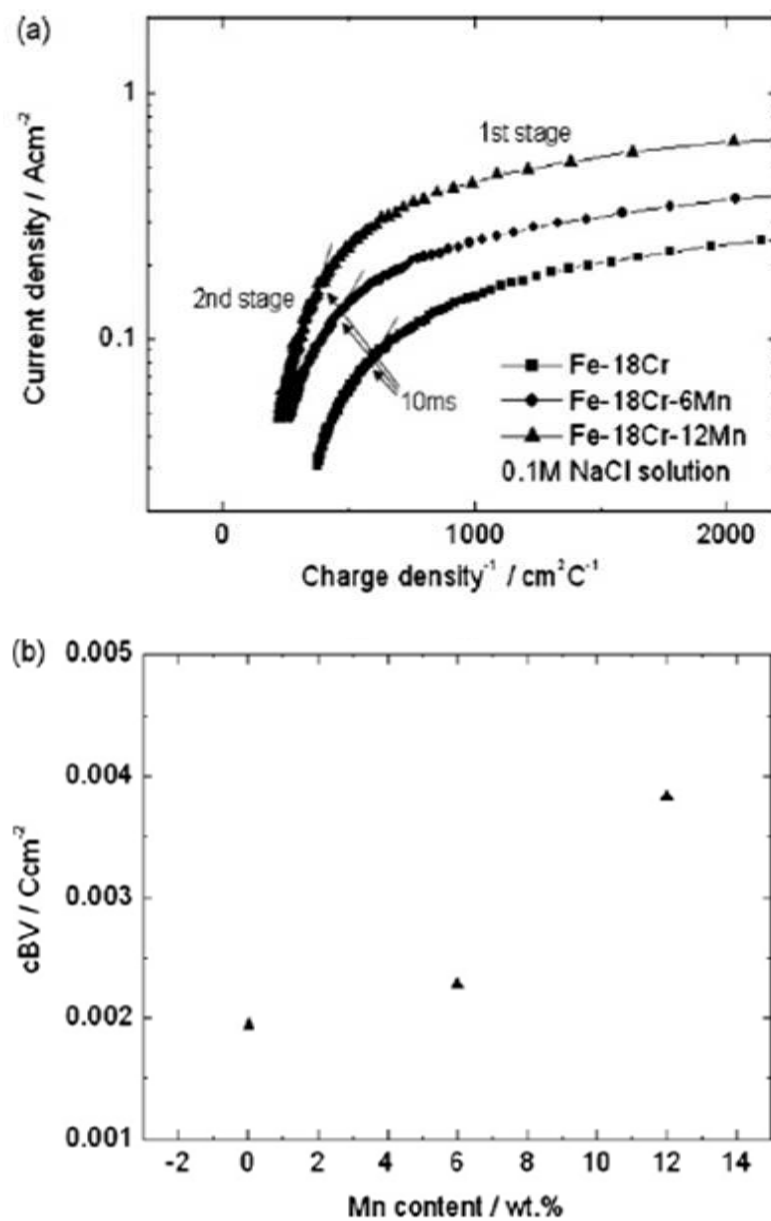


**Figure 6.** (a)  $\log i(t)$  vs.  $1/q(t)$  plots of Fe–18Cr–xMn ( $x = 0, 6, 12$ ) drawn based on the current transient curves in Fig. 5, and (b) the  $cBV$  values obtained from the slope of  $\log i(t)$  vs.  $1/q(t)$  plots. [Source: Ref. 45]

Fig. 6 (a) shows the  $\log i(t)$  vs.  $1/q(t)$  plots for Fe–18Cr–xMn ( $x = 0, 6, 12$ ) drawn based on the data in Fig. 5. After 10ms from the scratching (at the second stage), the relation between  $i(t)$  and  $q(t)$  evidently followed the HFM in which  $\log i(t)$  is linearly proportional to  $1/q(t)$ . According to HFM [26], a decrease in the activation energy barrier ( $E_a$ ) for ion movement through passive film under the

electric field is proportional to the product of B and V. Thus, the higher value of cBV provides a lower activation energy barrier for a movement of ion through the passive film, and hence facilitates the ion movement through the film. Since the ion conduction rate through the passive film is associated with the protectiveness of the film, an alloy with a higher value of cBV appears to reform a less protective film with faster ion conduction rate during the repassivation. In the  $i(t)$  and  $1/q(t)$  plots for Fe–18Cr–xMn ( $x = 0, 6, 12$ ), cBV obviously increased with Mn content, as presented in Fig. 6(b). From the results, it is evident that the increase in Mn content decreases the repassivation rate of the alloys, which will ultimately decrease their SCC resistance as was the case in case high Mn-N alloys investigated by Toor et al.[30].

In a recently published paper, Toor et al. [46] studied the effect of Si on SCC of SSs based on cBV model. They investigated the repassivation kinetics of alloy 304Si in which Si was intentionally added to increase its SCC resistance. There are studies which show that Si improves the localized corrosion resistance of the SSs by moving the pitting potential in the noble direction [47-51]. This increase in resistance to pitting corrosion of the Si-containing SSs alloys is due primarily to the change produced at grain boundaries by Si. Some others have suggested that Si increased stability of the passive state, resulting from an increase in the Si content of the protective film [52].

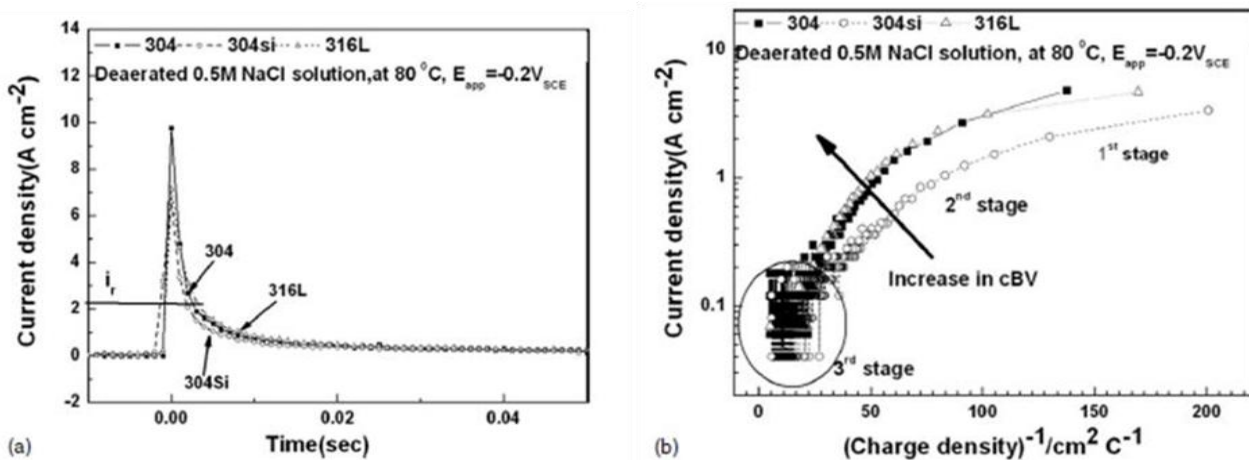


**Figure 7.** (a) Current transients for 304Si, 304, and 316L SSs, respectively, in deaerated 0.5 M NaCl at 80°C. (b) Log  $i(t)$  vs  $1/q(t)$  plots based on the data in (a). [Source: Ref. 46]

Results of 304Si were compared with that of 316L, and 304 alloys. Fig. 7(a) shows the current-time transients of the alloys 304Si, 304, 316L when a scratch was made on the surface of the alloys after a stable passive film had been formed at  $-0.2 \text{ V}_{\text{SCE}}$  at 80 °C in 0.5M NaCl solution at 80 °C. It was found that 304Si SS has the lowest peak current intensity among the alloys, which means Si decreased the oxidation tendency of 304 Si SS. The repassivation rate of an alloy can be compared by the repassivation time that has been passed to achieve the predetermined degree of repassivation from scratching. The shorter the repassivation time, the faster will be the repassivation rate of the alloy. In Fig. 7(a), it took a shorter time for 304Si SS to be repassivated to a predetermined degree of repassivation ( $i_r$ ). Figure 7(b) shows the comparison of the cBV values of the three alloys, and it is

clear that 304Si SS has the lowest cBV value when compared with other two alloys 316L, 304, which means that Si increases the repassivation rate of 304Si SS with formation of thinner and less protective passive film, and this will ultimately lead to higher SCC resistance of 304Si SS alloy than any other alloys and thus, SCC resistance of the alloys will be in the order of 304 Si > 304 > 316L. Results predicted by cBV model were further verified by conducting the SCC tests in boiling MgCl<sub>2</sub> solution for the three alloys as shown in Fig 8. Fig. 8(a) shows the load-elongation curves for the alloys when SSRT tests were conducted in 35 wt % MgCl<sub>2</sub> at 120°C. Elongation for all the alloys was significantly decreased on the order 304Si > 316L > 304. SEM fractographs show that 304 SS was fractured in a quasi-cleavage mode, a typical SCC fracture morphology of SS in a chloride solution (Fig. 8(b)), whereas 304Si failed in a ductile mode. 316L, however, failed by ductile fracture mode, partially mixed with quasi cleavage. Thus, the resistance to SCC of the alloys, when evaluated by the elongation prior to failure in the SSRT tests, is on the order of 304Si > 316L > 304.

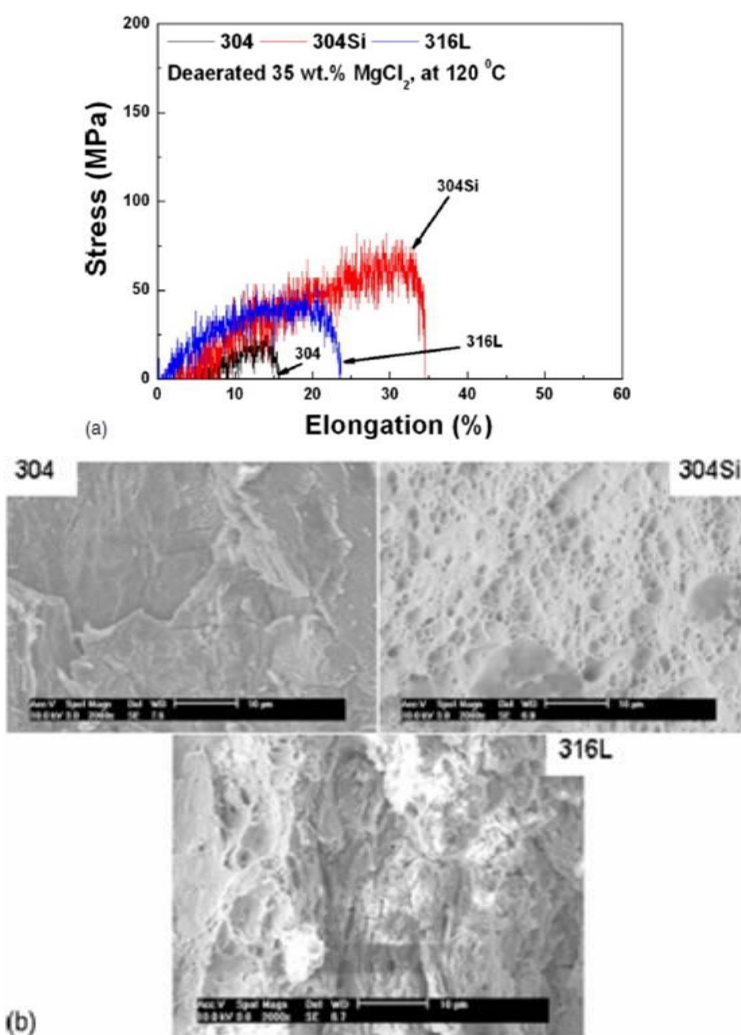


**Figure 8.** (a) Load elongation curves of the alloys in 35 wt % MgCl<sub>2</sub> at 120°C by SSRT and (b) SEM fractographs of the fractured samples at 120°C showing ductile fracture in 304Si, quasi-cleavage fracture in 304, and a ductile partially mixed with quasi cleavage in 316L. [Source: Ref. 46]

This cBV model was also successfully used to investigate the effect of inhibitors on repassivation kinetics [53] of alloy 600 in caustic solutions. Ni-base alloys are widely used in pressurized water reactors (PWR) as steam generator (SG) tubing materials, because of their excellent corrosion resistance and high temperature strength in aqueous environments. Despite of their exceptional general corrosion resistance, these alloys are susceptible to localized corrosion attack such as (SCC), corrosion fatigue and hydrogen assisted cracking. SCC on both primary and secondary side of the PWR has been considered a predominant degradation mode that leads to SG tubing failures [54] and the use of inhibitors is one of the intelligent approaches to mitigate SCC on secondary side of SG tubing in PWR. Extensive research has been carried out to develop and qualify inhibitors like  $\text{TiO}_2$ , which can be added to reduce SCC susceptibility and to extend the lifespan of already cracked SG tubing by decreasing the crack propagation rate [7, 11]. So in order to evaluate the effect, over saturated solution was prepared by adding 0.05 g/L of  $\text{TiO}_2$  powder in 10 % NaOH and mixed overnight. Specimens were cathodically cleaned at -1.0 V<sub>SCE</sub> for 5 min. and passivated for 1 h to make a stable passive film (at passive potential) during rapid scratch electrode test. After forming a stable passive film at 0.0 V<sub>SCE</sub> in pH 10 borate buffer solution at 90 °C, it was scratched under a potentiostatic condition. The results showed that peak current density ( $i_p$ ) value was decreased with  $\text{TiO}_2$  addition and cBV value was also decreased, i.e. addition of  $\text{TiO}_2$  increased the repassivation rate of the alloy by making a more protective and stable passive film on alloy surface as shown in Figs. 9(a) and (b) respectively.

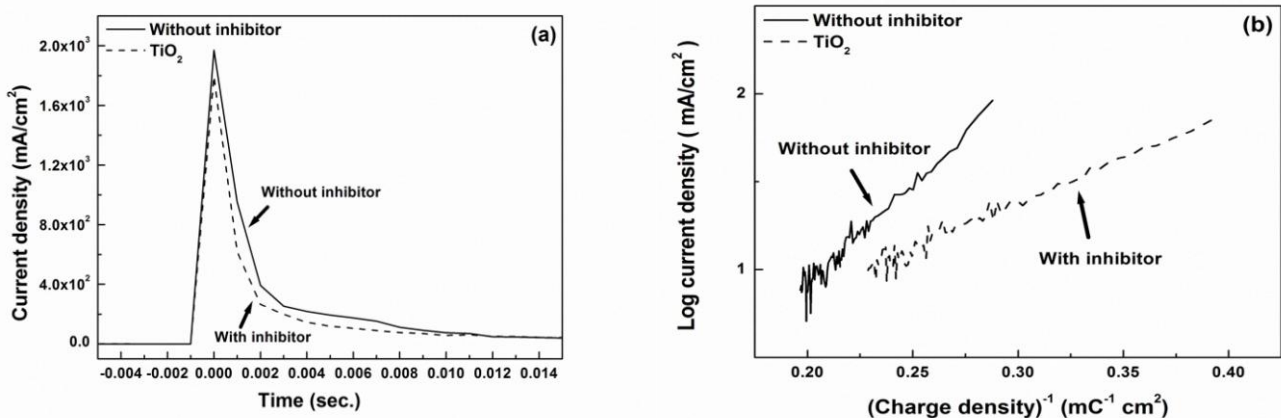


**Figure 9.** Current transients of scratched surface of Alloy 600 in the presence of  $\text{TiO}_2$  in (a) deaerated 10 % NaOH at 90 °C (b)  $\log i(t)$  vs.  $1/q$  plot based on Fig. 9(a). [Source: Ref. 53]

Bernard et al. [55] applied cBV model successfully to predict the SCC susceptibility of duplex stainless steel (DSS) 2205 alloy, which is widely used as a structural material in oil and gas production industries where high mechanical strength as well as corrosion resistance are required. The combination of ferrite and austenite phases in DSSs exerts a beneficial influence on the SCC properties in chloride environments [56, 57]. As repassivation kinetics is one of the approaches that has been extensively and successfully applied to interpret and predict SCC mechanisms for passive alloys [9, 28, 58], so it was used here for the investigations. Fig. 10 shows typical current transient curves when

a scratch was made on the surface of a specimen polarized to various applied potentials in range of  $-0.6$  to  $-0.1$  V<sub>SCE</sub> in 4 M NaCl at 90°C. It is evident that once the passive film was broken by scratching the surface of the alloy, the anodic current increases abruptly to a peak value due to an increase in anodic oxidation reaction on the bare surface, and thereafter decreases as repassivation proceeds. With an increase in applied potential, the current peak intensity increased due to an increased oxidation tendency at the bare metal. Except for the case of  $-0.1$  V<sub>SCE</sub>, repassivation occurred completely at different rates depending on applied potential. At  $-0.1$  V<sub>SCE</sub>, severe dissolution occurred as evidenced by an increase in current density after 20 ms. Anodic current measured on the scratched surface during repassivation is consumed for two anodic processes: metal dissolution and repassivation.

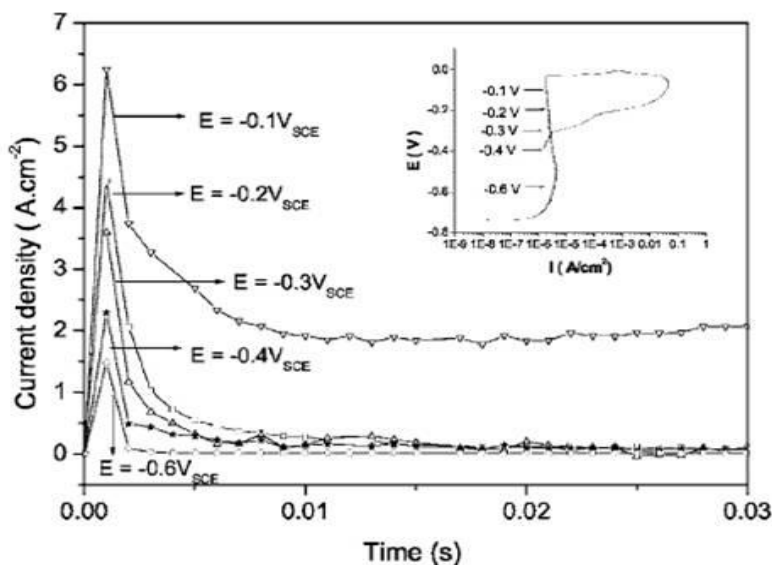


**Figure 10.** Effects of applied potentials on the current transients on scratched surfaces of DSS 2205 in 4 M NaCl at 90°C ( Inset of the figure shows applied potential used for the scratch test.) [Source: Ref. 55]

Marshall and Burstein [59, 27] demonstrated that for SS in chloride solution, the anodic current measured during repassivation is negligibly small, as long as the metal dissolution is not dominant by pitting or general corrosion.

Thus, except for the applied potential of  $-0.1$  VSCE, most of the anodic current flowing from the scratch in Fig. 10 is consumed for the formation of passive film. Based on the current transient curve obtained at  $-0.2$  V<sub>SCE</sub> in Fig. 10,  $\log i(t)$  vs charge density  $q(t)$  and the  $\log i(t)$  vs  $1/q(t)$  plots are shown in Figs. 11(a) and (b), respectively. Evidently, the current transient at the initial stage (11 ms) followed the place-exchange model [25] in which  $\log i(t)$  is linearly proportional to  $q(t)$ . In contrast, the current transient at the second stage, after 11 ms was driven by the high-field conduction model [26] in which  $\log i(t)$  is linearly proportional to  $1/q(t)$ . The influence of applied potentials on the  $\log i(t)$  vs  $1/q(t)$  plot is shown in Fig. 12 and it shows that the value of cBV increased with an increase in applied

potential and approached a limiting value at  $-0.2$  V<sub>SCE</sub>, beyond which an inflection point appeared in the log  $i(t)$  vs  $1/q(t)$  plot without further increase in cBV.

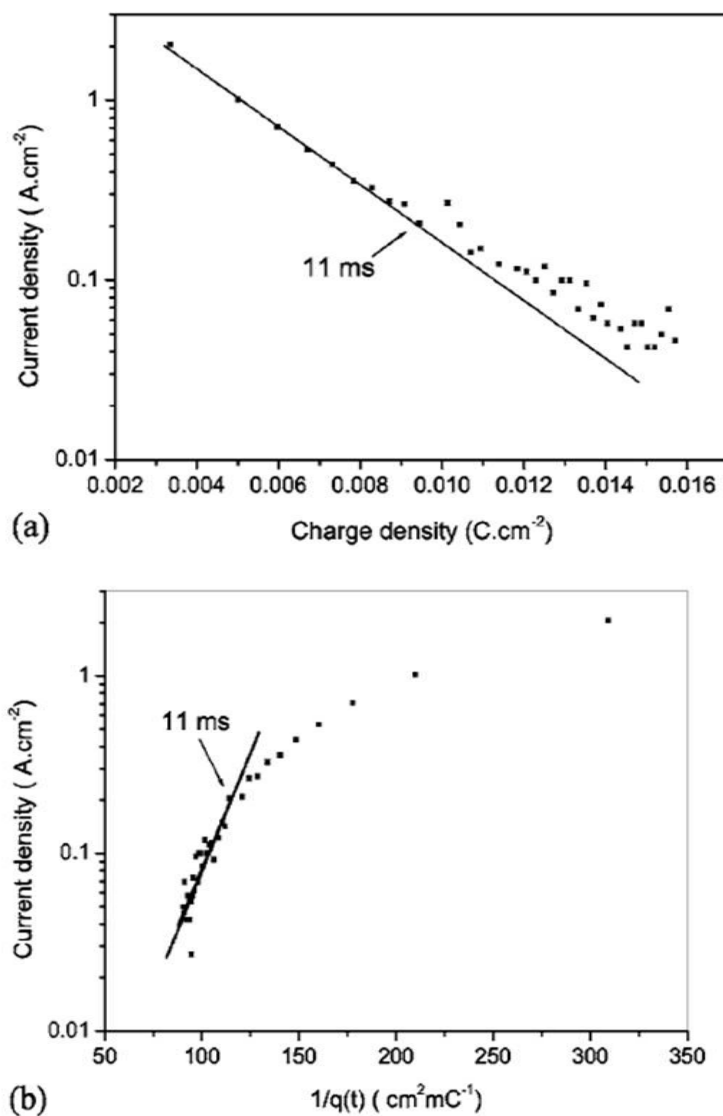


**Figure 11.** (a) Log  $i(t)$  vs  $q(t)$  and (b) log  $i(t)$  vs  $1/q(t)$  plots drawn based on the data in the current transient curve of DSS 2205 measured when a scratch was made at  $-0.2$  V<sub>SCE</sub> in 4 M NaCl at  $90^\circ\text{C}$ , as shown in Fig. 10. [Source: Ref. 55]

The results showed an increase in the cBV value with an increase in the applied potential means a slower repassivation rate with formation of thicker and less protective film at higher applied potential. So cBV model suggested an increase in SCC susceptibility of DSS with an increase in applied potential and these results were further verified by SSRT experiments as shown in Fig. 13. At potentials below  $-0.2$  V<sub>SCE</sub>, SCC did not occur as confirmed by the elongation greater than 30% that is comparable to that obtained from a tension test in air. At potentials noble to  $-0.25$  V<sub>SCE</sub>, the alloy appears to be failed by SCC or a severe dissolution, as shown by the significant reduction in the elongation. It is reported by Cho et al. [28] that repassivation rate in SSs increases with increasing the

contents of Cr, Mo, W and nitrogen content [58]. It is well known that Cr and Mo are enriched in ferrite, whereas Ni and N are in austenite in DSS.

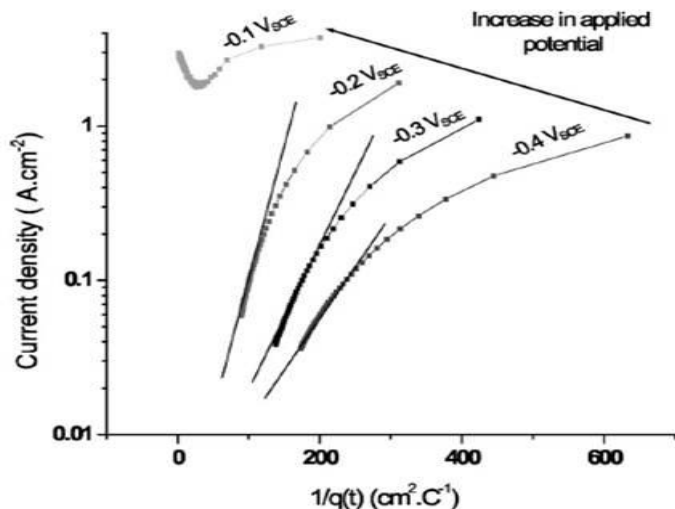


**Figure 12.** Effects of applied potential on the  $\log i(t)$  vs  $1/q(t)$  plot for DSS 2205 in 4 M NaCl solution at 90°C. [Source: Ref. 55]

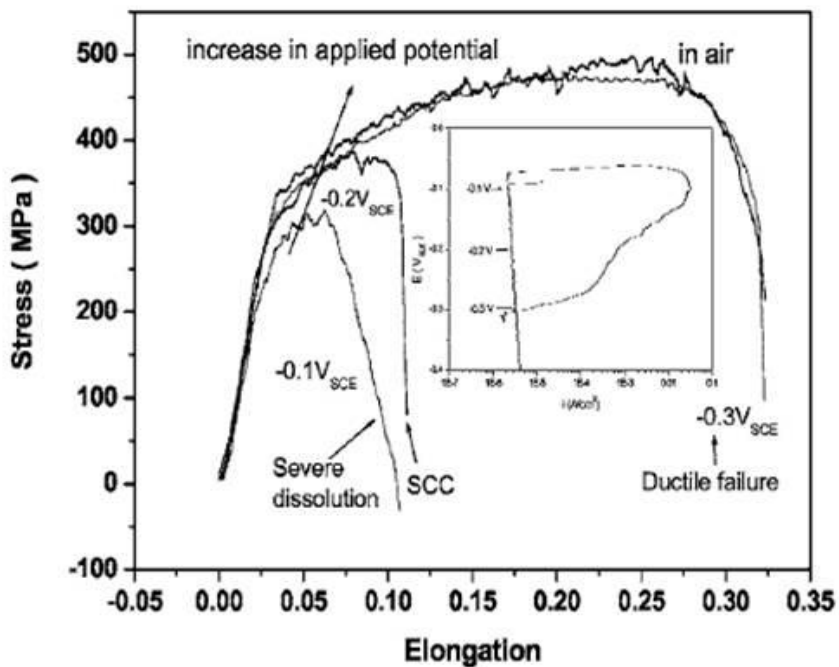


**Figure 13.** Effects of applied potential on the stress-strain curve of DSS 2205 straining at a rate of  $1.6 \times 10^{-6}$ /s in 4 M NaCl at 90°C. Inset of the figure shows applied potentials used in SSRT. [Source: Ref. 55]

Thus, the beneficial effects of Cr and Mo enriched in ferrite on the repassivation rate and those of nitrogen enriched in austenite may lead to the fact that there is no large difference in repassivation rate between the two phases in DSS. These effects with fine combination of the two phases in DSS

appear to produce repassivation kinetics that resembles that of austenitic SS or that of ferritic SS. By comparing the cBV data with SSRT results in Fig. 13, the change in cBV value can be correlated with SSRT results.

SeJin et al. [60] used cBV model to investigate the SCC susceptibility of alloy 690 in high temperature containing small amount of Pb compounds. Alloy 600, widely used as a heat exchanger tube material in nuclear power plants, has experienced intergranular stress corrosion cracking (IGSCC) and intergranular attack (IGA) from either the primary side or the secondary side of steam generators. From the recognition that it is necessary to increase Cr contents in alloy 600 to enhance the IGSCC resistance, alloy 690, with chemical compositions of Ni-30Cr-10Fe, was developed and now replaces alloy 600 for stream generator tube. It has been known that SCC of alloy 600 and alloy 690 in secondary side of steam generators occurs mainly in high temperature caustic solution or in S containing solutions such as  $H_2S_xO_6$  and  $Na_2S_2O$ . However, lead is now being considered as a new origin of SCC of alloy 600 and alloy 690. Lead compounds have been detected in the secondary side of more than 30 nuclear power plants worldwide [61-64]. There have been some previous reports on lead-induced SCC of these alloys including the effects of alloying elements, micro-structure and lead chemicals on SCC resistance [65-67], however the mechanism of lead-induced SCC of Ni-based alloy is still not clear, so cBV model was applied to investigate SCC susceptibility of this material. Analytical grade PbO was used to make required concentration (ppm) of Pb in the solutions.

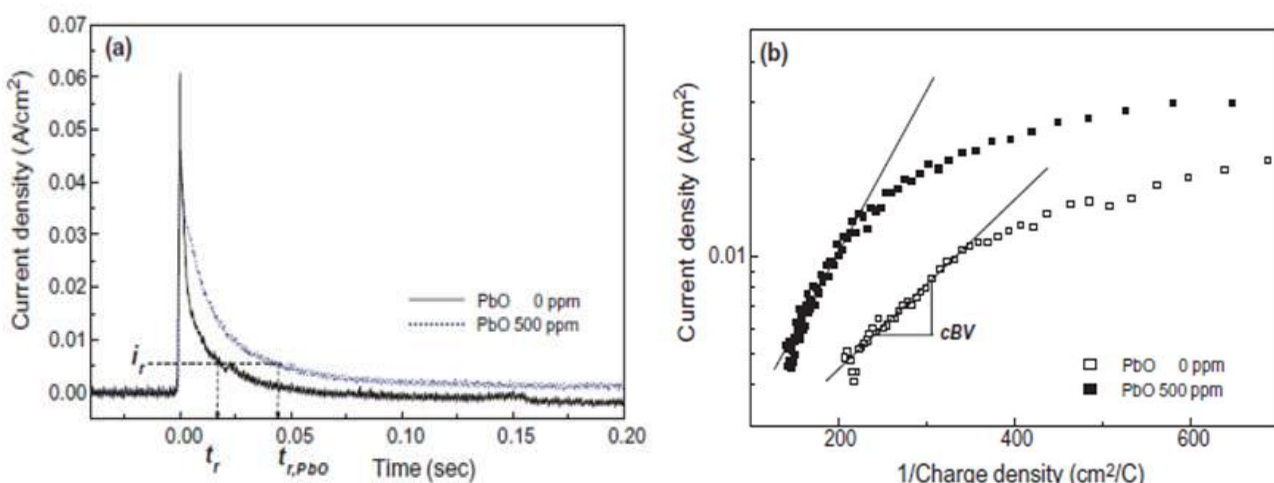


**Figure 14.** (a) Current transient curves and (b)  $\log i(t)$  vs.  $1/q(t)$  plots of alloy 690 in  $90^0\text{C}$ , pH 4 water at an applied potential of  $-0.1 \text{ V}_{\text{SCE}}$ . [Source: Ref. 60]

Fig. 14 shows the current transient curves for alloy 690 in pH 4 water (without and with addition of PbO). The anodic current density of the alloy is clearly higher in solutions without PbO than those with PbO. In Fig. 14(a) it took shorter time,  $t_r$ , for alloy to repassivate to the predetermined degree of repassivation ( $i_r$ ) in the PbO-free solution than that in the PbO-containing solution,  $t_{r,PbO}$ . They found that the repassivation rate of alloy 690 is decreased by the addition of PbO in solutions. Log  $i(t)$  vs.  $1/q(t)$  plots showed in Fig. 14(b) a higher value of cBV in solutions containing PbO than

those without PB, which means that repassivation rate of the alloy becomes slower with addition of PbO. Consequently, SCC resistance of the alloy will be lower in the PbO-containing solutions than in PbO-free solutions. These results support the work of previous researchers, who claimed that the lead-induced SCC of Ni-based alloy occurs mainly in alkaline environments [68-70]. Therefore, the reason for the decrease in SCC resistant of alloy 690 in a solution contaminated with lead is due presumably to the decrease in the repassivation rate of the alloy.

#### 4. CONCLUSIONS

Based on this review it can be concluded that SCC susceptibility of passive materials is closely related with their repassivation kinetic behavior which can be investigated using RSET. cBV value determined from the slope of the ( $\log i(t)$  vs.  $1/q(t)$ ) plot is very effective as a measure of repassivation rate and hence is associated with SCC susceptibility. For an alloy/environment system, the lower the value of cBV, faster will be the repassivation rate of that alloy with more protective film and this will ultimately decrease its SCC susceptibility.

#### ACKNOWLEDGEMENTS

The author gratefully acknowledges the support provided by King Fahd University of Petroleum & Minerals (KFUPM), Saudi Arabia in conducting this research work under the research grant #IN121033.

#### References

1. D. D. Macdonald, *Pure Appl. Chem.*, 71, 6 (1999) 951
2. H. H. Uhlig, Passivity of Metals, The Electrochem. Soc., Princeton, NJ (1978) 1
3. D. D. Macdonald, *J. Electrochem. Soc.*, 139 (1992) 3434
4. P. Schmuki and H. Bohni, *Werkst. Korros.*, 42 (1991) 203
5. J.C. Scully, in: Z.A. Frououlis (Ed.), Environment Sensitive Fracture of Engineering Materials, AIME, New York (1979) 71
6. R.W. Staehle, Stress Corrosion Cracking and Hydrogen Embrittlement of Iron Base Alloys, NACE, Houston (1977) 180
7. D. H. Hur, J. S. Kim, J. S. Baek and J. G. Kim, *Corrosion* 58 (2002) 1031
8. R. Bandy, R. Roberge and D. van Rooyen, *Corrosion* 41 (1985) 142
9. H.S. Kwon, E.A. Cho and K.A. Yeom, *Corrosion*, 56(2000)32
10. B. P. Miglin and J.P. Paine, Proceeding of 6th International Symposium on Environmental Degradation of Materials in Nuclear Power-systems Water reactors, San Diego, CA(1993) 303
11. U. C. Kim, K. M. Kim, J. S. Kang, E. H. Lee and H. P. Kim, *Journal of Nuclear Materials* 302 (2002)104
12. J. C. Scully, *Corros. Sci.*, 20 (1980)997
13. T. Nakayama, M. Takano, *CORROSION*, 42(1986)10
14. M. Barbosa, *CORROSION*, 40 (1988) 149
15. Parkins, R.N., "Development of strain rate testing and its implications", ASTM STP 665 (1979)5

16. Diegle, R.B. and Boyd, W.K., "The role of film rupture during slow strain rate stress corrosion cracking testing", *ASTM STP 665* (1979)24
17. P. Engseth and J.C. Scully, *Corros. Sci.* 15 (1975) 505
18. X.G. Zhang and J. Verrecken, *CORROSION*, 45 (1989) 57
19. T. Kodama and J.R. Ambrose, *CORROSION*, 33 (1977) 155
20. S.I. Pyun and M.H. Hong, *Electrochim. Acta*, 37 (1992) 2437
21. T.R. Beck, *Electrochim. Acta*. 18 (1973) 815
22. R.C. Newman, *Corros. Sci.* 25 (1985)331
23. P.I. Marshall and G.T. Burstein, *Corros. Sci.* 24 (1984) 463
24. F.J. Graham, H.C. Brookes and J.W. Bayles, *J. Appl. Electrochem.* 20 (1990) 45
25. N. Sato and M. Cohen, *J. Electrochem. Soc.* 111 (1964)512
26. N. Cabrera and N. F. Mott, *Rep. Prog. Phys.* 12 (1948)163
27. G. T. Burstein and P. I. Marshall, *Corros. Sci.* 23 (1983)125
28. E. A. Cho, J. K. Kim, J. S. Kim and H. S. Kwon, *Electrochim. Acta*, 45 (2000) 1933
29. K. A. Yeom, E. A. Cho, H. S. Kwon and J. J. Kim, *Materials Science Forum* 289-292 (1998) 969.
30. I.H. Toor, K.J. Park and H.S. Kwon, *J. Electrochem. Soc.* 154 (2007) C494
31. R. Merello, F. J. Botana, J. Botella, M. V. Matres, and M. Marcos, *Corros. Sci.*, 45 (2003) 909
32. Y. H. Jang, S. S. Kim, and J. H. Lee, *Mater. Sci. Eng.*, A, 396 (2005)302
33. C. D. Van Lelyveld and A. Van Bennekom, *Mater. Sci. Eng.*, A, 205(1996) 229
34. M. Kemp, A. van Bennekom, and F. P. A. Robinson, *Mater. Sci. Eng.*, A, 199(1995) 183
35. R. L. Klueh, P. J. Maziasz, and E. H. Lee, *Mater. Sci. Eng.*, A, 102(1988) 115
36. R. D. Knutsen, C. I. Lang, and J. A. Basson, *Acta Mater.*, 52 (2004) 2407
37. C.-M. Tseng, H.-Y. Liou, and W.-T. Tsai, *Mater. Sci. Eng.*, A, A344 (2003) 190
38. V. Mitrovic-Scepanovic, R.J. Brigham, *Corrosion* 52 (1996) 23
39. J.O. Park, T. Suter, H. Bohni, *Corrosion* 59 (2003) 59
40. N.J.E. Dowling, C. Duret-Thual, G. Auclair, J.P. Audouard, P. Combrade, *Corrosion* 51 (1995) 343
41. E.G. Webb, T. Suter, R.C. Alkire, *J. Electrochem. Soc.* 148 (2001) B186
42. 14. R. A. Lula and W. G. Renshaw, *Met. Prog.*, (1965) 69
43. J. S. Stanko and D. Wellbeloved, *Manganese in Corrosion Resistant Steel*, Report SAMANCOR, Ltd., Johannesburg, South Africa, (1991)10
44. E. Lunarska, Z. Szklarska-Smialowska, and M. Janik-Czachor, , *CORROSION*, 31 (1975)7
45. K.J. Park and H.S. Kwon, *Electrochim. Acta* 55 (2010)3421
46. I.H.Toor, J. Y. Kwon and H.s. Kwon, *J. Electrochem. Soc.* 155 (2008)C495
47. M. Pourbaix, *Atlas of Electrochemical Equilibrium in Aqueous Solutions*, p. 461, Pergamon Press, London (1966)
48. F. H. Scott, G. C. Wood, and J. Stringer, *Oxid. Met.*, 113(1995) 145
49. S. N. Basu and G. J. Yurck, *Oxid. Met.*, 281(1991)315
50. M. A. Streicher *J. Electrochem. Soc.*, 103 (1956)375
51. A. J. Sedriks, , *CORROSION*, 42 (1986)376
52. T. N. Rhodin, , *CORROSION*, 12 (1956)123
53. I.H.Toor, M.Ejaz and H.S.Kwon, *CORROSION*, 69 (2013)590
54. D. R. Diercks, W. J. Shack and J. Muscara, *Nuclear engineering and design* 194 (1999) 19
55. F. Bernard, V. S. Rao, and HS Kwon, *Journal of The Electrochemical Society*, 152 ,Vol.10(2005) B415
56. J. Hochmann, A. Desestret, P. Jolly, and R. Mayoud, in Stress Corrosion Cracking and Hydrogen Embitterment of Iron Base Alloys, R. W. Staehle, J. Hochmann, R.cD. McCright, and J. E. Slater, Editors, NACE, Houston, TX (1977)956
57. N. Sridhar, J. Kolts, S. K. Srivastava, and A. L. Asphahani, in Duplex Stainless Steels, R. A. Rula, Editor, American Society for Metals, Metals Park, OH(1983)481
58. J.-W. Park, V. Shankar Rao, and H. S. Kwon, *CORROSION*, 60(2004) 1099

59. P. I. Marshall and G. T. Burstein, *Corros. Sci.*, 23(1983)1219
60. S.J. Ahn, V. S. Rao, H.S. Kwon and U.C. Kim, *Corros. Sci.*, 48(5) (2005)1137
61. A.K. Agrawal, J.P.N. Paine, in: Proceedings of the 4th International Symposium on Environmental Degradation of Materials in Nuclear Power Systems—Water Reactor, August 6–10, 1989, Jekyll Island, Georgia, p. 7-1 (NACE, Houston, USA, 1990).
62. B.P. Miglin, J.M. Sarver, in: Proceedings of the 4th International Symposium on Environmental Degradation of Materials in Nuclear Power Systems—Water Reactor, August 6–10, 1989, Jekyll Island, Georgia, p. 7–18 (NACE, Houston, USA, 1990).
63. B.P. Miglin, J.M. Sarver, in: Proceedings of the 5th International Symposium on Environmental Degradation of Materials in Nuclear Power Systems—Water Reactor, August 25–29, 1991, Monterey, California, p. 757 (ANS, La Grange Park, USA, 1992).
64. A. Rocher, F. Cattant, D. Buisine, B. Prieux, M. Helie, in: Proceedings of the Contribution of Materials Investigation to the Resolution of Problems Encountered in PWRs, Fontevraud III, September 12–16, 1994, p. 537 (SFEN, France, 1994).
65. J.M. Sarver, in: Proceedings of the 1987 EPRI Workshop on Secondary-side Intergranular Corrosion Mechanisms, vol. 2, EPRI NP-5971, September, 1988, p. C11.
66. F. Vaccaro, in: Proceedings of the 1987 EPRI Workshop on Secondary-side Intergranular Corrosion Mechanisms, vol. 2, EPRI NP-5971, September, 1988, p. C12.
67. T. Sakai, T. Senjuh, K. Aoki, T. shigemitsu, Y. Kiah, in: Proceedings of the 5th International Symposium on Environmental Degradation of Materials in Nuclear Power Systems—Water Reactor, August 25–29, 1991, Monterey, California, p. 764 (ANS, La Grange park, USA, 1992).
68. M. Helie, I. Lambert, G. Santarini, in: Proceedings of the 7th International Symposium on Environmental Degradation of Materials in Nuclear Power Systems—Water Reactor, August 7–10, Breckenridge, Colorado, p. 247, 1995 (NACE, Houston, 1995).
69. W. Staehle, in: Proceedings of the 1st International Conference on Environmental- induced Cracking of Metals, Kohler, WI, USA, Oct. 2–7, 1988 (NACE, Houston, 1990).
70. A.M. Lancha, M. Garcia, M. Gernandez, in: Proceedings of the International Conference on Chemistry in Water Reactor, Nice, France, April 24–27, 1994 (SFEN, 1994).